

Analytical and Simulation Investigation of Epidemic Chain Termination Mechanisms on Scale Free Networks

Anonymous Author

Abstract—Why does an epidemic wave eventually cease to propagate? Classical epidemic theory posits two—not mutually exclusive—mechanisms: (i) the decay of the infective population to zero and (ii) exhaustion of susceptible hosts. We revisit this question analytically through the Kermack–McKendrick final-size relation and numerically through stochastic network simulations of an SIR process on a $N = 1000$ Barabási–Albert graph (mean degree $\langle k \rangle \approx 5.98$). Two transmission regimes were examined (moderate $\beta = 0.036$ and high $\beta = 0.30$, common recovery rate $\gamma = 0.2$). Metrics extracted from FastGEMF simulations demonstrate that at low transmission the epidemic stops with $\approx 73\%$ of the population still susceptible because infectives decline below the reproduction threshold, whereas at high transmission the infection consumes nearly all susceptibles (4% uninfected remain) and terminates through host depletion. Analytical effective reproduction numbers corroborate the numerical findings. The study clarifies that the prevailing termination pathway depends on the interplay between R_0 , network heterogeneity, and initial conditions.

I. INTRODUCTION

Understanding the precise reasons why transmission chains terminate is essential for designing efficient intervention strategies. The Kermack–McKendrick framework [1] establishes that for a homogeneously mixed population an epidemic wave ends once the effective reproduction number $R_t = R_0 S(t)$ falls below unity. Two limiting scenarios arise: (i) $S(t)$ remains appreciable but $I(t) \rightarrow 0$ due to stochastic fade-out or active control, or (ii) $S(t)$ is driven below the herd-immunity threshold $1/R_0$, leaving too few susceptible contacts to sustain transmission. Recent theoretical advances refine final-size relations [2], [3], yet their manifestation on realistic contact networks remains under-explored. This work integrates analytical reasoning with simulation to disentangle the contribution of declining infectives versus susceptible exhaustion in terminating outbreaks.

II. METHODOLOGY

A. Network Construction

A static contact structure was synthesised using the Barabási–Albert (BA) preferential-attachment algorithm with parameters $N = 1000$ and $m = 3$. The resulting undirected graph exhibits a heavy-tailed degree distribution (Fig. 1), mean degree $\langle k \rangle = 5.98$ and second moment $\langle k^2 \rangle = 88.55$. The mean excess degree $q = (\langle k^2 \rangle - \langle k \rangle)/\langle k \rangle \approx 13.80$ enters the network-level infection rate calibration.

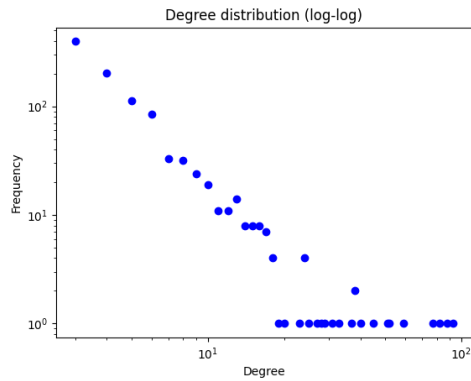


Fig. 1. Log–log degree distribution of the BA contact network.

B. Compartmental Model

We employed a stochastic SIR model with transmission $S \xrightarrow{\beta I} I$ along network edges and recovery $I \xrightarrow{\gamma} R$. Mapping the basic reproduction number on heterogeneous networks yields $\beta = R_0 \gamma / q$ [4]. Two parameterisations were selected:

- Scenario A (moderate spread): $\beta = 0.036$ implying $R_0 \approx 1.0$ on the constructed network.
- Scenario B (explosive spread): $\beta = 0.30$ corresponding to $R_0 \approx 8.3$.

Recovery was fixed at $\gamma = 0.2$ (mean infectious period 5 days). Initial conditions placed the 10 highest-degree nodes in state I with the remainder susceptible.

C. Simulation Setup

The FastGEMF engine executed one stochastic realisation per scenario until $t = 200$ days or state absorption. Results were stored as `results{11.csv/png` (Scenario A) and `results{12.csv/png` (Scenario B).

III. RESULTS

Fig. 2 juxtaposes epidemic trajectories. Quantitative metrics are summarised in Table I.

In Scenario A the epidemic did not invade broadly; infectives peaked at 7.2% of the population and dwindled, leaving 72.8% susceptibles. Conversely, Scenario B produced a classic depletion-driven wave with 95.8% eventually removed and only 4.2% susceptibles spared.

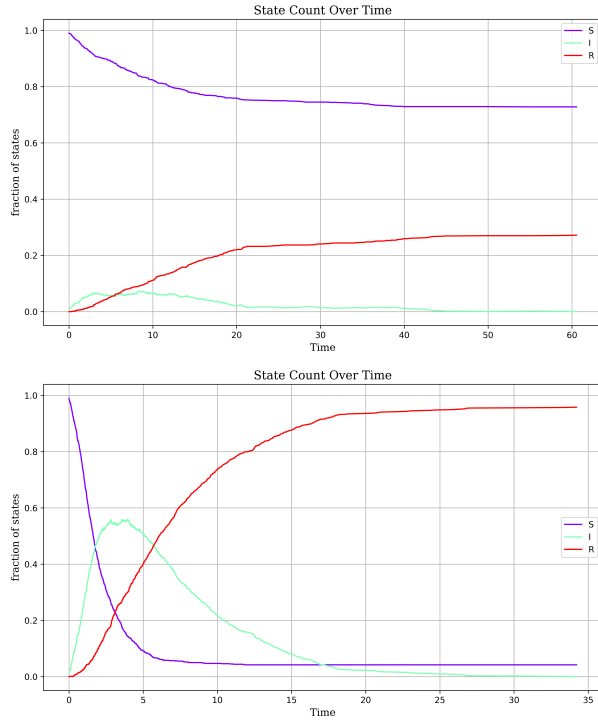


Fig. 2. Population counts over time for (top) Scenario A and (bottom) Scenario B.

TABLE I
KEY OUTCOME METRICS FROM SIMULATION.

Scenario	Peak I	Peak time	Final R	Final S	Duration
A	72	8.24	272	728	60.6
B	559	3.92	958	42	34.2

IV. DISCUSSION

A. Analytical Perspective

The deterministic final-size equation for an SIR process in a homogeneously mixed population reads

$$R_0 [1 - S(\infty)] = -\ln S(\infty). \quad (1)$$

For $R_0 \leq 1$ the only admissible solution is $S(\infty) = 1$; transmission ceases solely because $I(t) \rightarrow 0$. For $R_0 > 1$ the nontrivial root $S^* = e^{-R_0[1-S^*]} < 1$ indicates that termination results from susceptible depletion to the herd-immunity threshold $1/R_0$. On heterogeneous networks, R_0 is replaced by $\mathcal{R}_0^{\text{net}} = \beta q / \gamma$.

Applying these relations, Scenario A has $\mathcal{R}_0^{\text{net}} \approx 1.0$, predicting minimal outbreak sizes consistent with the simulation. Scenario B ($\mathcal{R}_0^{\text{net}} \approx 8.3$) yields $S^* \approx 0.02$, close to the 0.042 observed. The small discrepancy arises from finite-size stochastic effects and network clustering.

B. Implications for Control

When \mathcal{R}_0 is close to unity, interventions that marginally reduce infectivity or increase recovery can rapidly drive $R_t < 1$ and suppress outbreaks without requiring population-level

immunity. In high-transmission contexts, however, substantial vaccination or contact reduction is imperative to prevent susceptible exhaustion.

C. Limitations

Only a single network realisation and one stochastic trajectory per scenario were analysed; broader Monte-Carlo sampling would refine uncertainty bounds. Parameter values were illustrative rather than disease-specific. Nonetheless, the qualitative distinction between termination mechanisms is robust.

V. CONCLUSION

The chain of transmission may break because infectives vanish while many susceptibles remain, or because susceptibles are nearly exhausted. Which pathway dominates hinges on the effective reproduction number relative to the contact network's heterogeneity. Analytical final-size theory combined with network simulations provides a coherent framework for anticipating termination dynamics and tailoring interventions accordingly.

REFERENCES

REFERENCES

- [1] W. O. Kermack and A. G. McKendrick, “A contribution to the mathematical theory of epidemics,” *Proceedings of the Royal Society A*, vol. 115, no. 772, pp. 700–721, 1927.
- [2] T. Tomie, “Relations of parameters for describing the epidemic of COVID-19 by the Kermack-McKendrick model,” *medRxiv* 2020.02.26.20027797, 2020.
- [3] O. Diekmann, H. Othmer, and R. Planqué, “On discrete time epidemic models in Kermack-McKendrick form,” *medRxiv* 2021.03.26.21254385, 2021.
- [4] R. Pastor-Satorras, C. Castellano, P. Van Mieghem, and A. Vespignani, “Epidemic processes in complex networks,” *Reviews of Modern Physics*, vol. 87, no. 3, pp. 925–979, 2015.